Article

Low Free Energy Barrier for Ion Permeation Through Double-Helical Gramicidin

Shirley W. I. Siu, and Rainer A Bo#ckmann

More About This Article

Additional resources and features associated with this article are available within the HTML version:

- Supporting Information
- Access to high resolution figures
- Links to articles and content related to this article
- Copyright permission to reproduce figures and/or text from this article

View the Full Text HTML

Low Free Energy Barrier for Ion Permeation Through Double-Helical Gramicidin

Shirley W. I. Siu and Rainer A Böckmann*

*Theoretical and Computational Membrane Biology, Center for Bioinformatics, Saarland University,
P.O. Box 15 11 50, 66041 Saarbrücken, Germany*

The pentadecapeptide gramicidin forms a cation-specific ion channel in membrane environment. The two main conformations are the head-to-head helical dimer (HD) known as the channel conformation and the intertwined double helical form (DH) often refer to as nonchannel conformation. In this comparative study, the energetics of single potassium ion permeation by means of the potential of mean force (PMF) for both gramicidin conformations embedded in a DMPC bilayer has been addressed by molecular dynamics simulations. A significantly decreased free energy barrier by ≈25 kJ/mol for potassium ion passage through DH as compared to HD is reported. Favorable electrostatic side chain-cation interactions in HD are overcompensated by phospholipid-cation interactions in DH. The latter are coupled to an increased accessibility of the channel entrance in DH due to distributed tryptophans along the channel axis. This result underscores the importance of the lipid environment of this channel not only for the equilibrium between the different conformations but also for their function as cation channels.

Introduction

Gramicidin A (gA) is the major component of the antibiotic gramicidin from the soil bacteria *Bacillus brevis*. Each monomer is made up of 15 alternating L- and D-amino acids capped at the two ends by a formyl group and an ethanolamine group. When dimerized, gA functions as a cation-selective transmembrane channel. In contrast to most structurally resolved ion channels, the unique sequence of the gA peptide is able to adopt a wide range of conformations based on various environmental factors, such as solvent history (incorporating solvents used to cosolubilize gramicidin and phospholipids), peptide concentration, types of lipids, temperature, and binding of cations.[1–6] Mainly, 2-folding motifs of gramicidin were reported in experimental structural studies, namely the single-stranded head-to-head helical dimer (HD)[7,8] and the double-stranded helical dimer (DH) (Figure 1),[6,9] which can be further categorized according to their handedness. In the past three decades, extensive experimental measurements were performed to discriminate the biological active conformation in the membrane from the nonactive one, and the head-to-head dimer has been considered as the concensus model (for reviews, see refs 10–12).

An important argument for the existence of head-to-head dimerization in membranes was given by Urry et al.[13] who showed that the dimers with covalently linked N-termini displayed conductivity. Bamberg et al. and Apell et al.[14,15] showed that modification at the N-terminus of the peptide but not at the C-terminus affected the single channel conductivity. Shift reagent NMR experiments indicated that both N-termini of the dimer were buried deeply within the bilayer while the C-termini were located near the surface of the membrane.[16] Furthermore, the circular dichronism spectrum (CD) of the channel embedded in a bilayer[17] was found to be qualitatively different from the spectrum obtained from channels in various organic solvents, in which the double helical dimer conformation
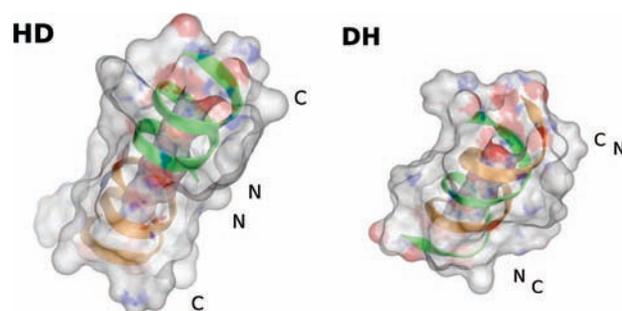

Figure 1. The two major conformations of gramicidin drawn in its solvent accessible surface (water radius 1.4 Å): the head-to-head (HD) and double-helical dimer (DH). The figure was prepared using Pymol.[85]

is predominant. Thereafter, CD spectra were conventionally used in laboratories to validate the peptide conformation in the samples.

While the head-to-head dimer was believed to be the thermodynamically more stable form in membrane environment, some experiments demonstrated that the peptide might as well adopt a conformation different from the HD structure by virtue of a different incorporation protocol. Using CD, Killian[1] observed that gramicidin prepared in ethanol preserved the antiparallel double-helical dimer conformation in the membrane. At room temperature, conversion to the HD form was very slow and thus the membrane was regarded as an environment of minimal conversion. Applying the High-Performance Liquid Chromatography, Bano[3] demonstrated that the double-stranded dimer coexists with the single-stranded form in the membrane in certain ratio. The finding of a right-handed double-stranded helical dimer conformation that showed agreement with the measured ^{15}N NMR pattern[9] again arose disputes[18–20] on the biologically active conformation of gramicidin in a lipid environment.

Despite the ongoing controversies, due to its small size and the well-defined channel pore gramicidin has been a popular

* To whom correspondence should be addressed. E-mail: rainer@bioinformatik.uni-saarland.de.

model system for studying the properties of an ion channel and the mechanism of ion conduction. Previous computational studies focused on the energetics of ion and proton permeation through the HD dimer. They cover continuum electrostatics calculations (see for example refs 21−24), semimicroscopic models,[25−27] as well as microscopic models.[28−36] The latter are particularly interesting for the level of detail which can be obtained. Potentials of mean force (PMF) for ion permeation through the HD channel derived from classical atomic-detail molecular dynamics (MD) showed an unexpectedly high central energy barrier and relatively weak binding sites at the channel entrances. Improved PMF profiles in reasonable agreement to observables could be obtained by correcting for system boundary and polarization effects.[25,31] Nevertheless, resulting barrier for potassium ion through HD is still in the range of 25 kJ/mol,[31] at least a factor of 2 too large compared to the experimentally derived barrier.[23]

On the other hand, the DH conformation hardly studied in simulations has been shown to translocate a water column at an increased rate as compared to HD.[37,38] The double-stranded conformation allows for an orientation of channel water dipoles favorable to a cation entry on both sides. Spontaneous water dipole restoration observed after ion passage suggested a facilitation of multiple ion passages in the DH as compared to HD.[38]

Here, in a comparative study we focus on the ion conduction properties of both DH and HD conformations using a nonpolarizable force field. The potential of mean force for one-ion permeation through the channel is computed. Our results reveal a decreased free energy barrier and an increased structural flexibility for DH as compared to HD. While the PMF profiles might be sensitive to the force field parameters, tests using a modified ion-protein interaction retained a decreased PMF barrier for the DH channel.

Methods

System Setup. The gramicidin embedded membrane system was prepared by the same procedure as described in our previous work.[38] It consists of a gramicidin, 124 dimyristoylphosphatidylcholine (DMPC) lipids and 6142 water molecules. The initial structures of gramicidin were taken from the PDB database: 1MAG[39] for the head-to-head helical dimer (HD) and 1AV2[9] for the intertwined double helix (DH). The system was equilibrated for 40 ns. The average area per lipid was approximately 60 Å^2, which is in agreement with experiment.[40] Bulk water molecules were replaced by K$^+$ and Cl$^-$ ions to achieve an ionic concentration of 200 mM. The system was further equilibrated to prepare for the free energy simulations.

Potential of Mean Force Calculations. The potential of mean force (PMF)[41] of ion permeation is the Helmholtz free energy W defined from the average distribution function of the sampled ion along the chosen permeation path ξ, in reference to the bulk value[42]

$$W(\xi) = W(\xi_0) - kT \ln\left[\frac{\langle\rho(\xi)\rangle}{\langle\rho(\xi_0)\rangle}\right] \quad (1)$$

For the PMF of ion permeation, the ion's positions along the gramicidin channel have to be sampled. Since ion permeation is a process with an activation barrier well above 1.5 k_BT,[23] classical MD simulations would yield an insufficient sampling. One way to circumvent this is to employ the umbrella sampling technique; by introducing a biased potential, the ion movement

is restrained to positions along the reaction pathway. The PMF is then calculated by unbiasing and combining the ion density distributions of the window simulations using the weighted histogram analysis method (WHAM) (see refs 42 and 43 for a review). The coordinate parallel to the bilayer normal was chosen as the reaction coordinate, and the protein's center of mass as the origin. The entire pathway covering the range of [−30, 30] Å was divided into 0.5 Å intervals summing up to a total of 121 windows.

To ensure similar starting conditions for the window simulations, we selected a trajectory from the classical simulations such that both the channel tilting angle and the channel length were equilibrated. For HD, convergence was reached in 20 ns (protein mean rms 0.15 nm, tilt angle 15.8 ± 2.5°, channel length 2.0 ± 0.02 nm) and for DH in 24 ns (protein mean rms 0.19 nm, tilt angle 5.0 ± 2.2°, channel length 1.6 ± 0.02 nm). The increased tilting of HD as compared to DH can be attributed to its increased channel length. The tilt enables polar interactions of the channel terminal tryptophans with the lipid hydrophilic headgroup region.

Starting structures for the window sampling were selected from the last 5 ns of the equilibration based on the following criteria: (a) the channel must be filled with water molecules and (b) a water molecule is found close to the center of the window (typically within 0.1 Å distance). The water molecule closest to the center of the respective window was exchanged with a potassium ion in the bulk. Throughout the unbiased simulations, both the HD and DH channel were partially closed by a nearby lipid. Similar headgroup protrusions were reported previously in other MD studies of the HD conformation of gramicidin using different types of lipids.[35,44] In order to obtain starting structures for windows in the channel entrance region, we performed additional classical simulations exchanging the water molecule in the single-file close to the blocked entrance with a potassium ion. The inserted ion escaped from the channel within about 2 ns simulation time for the HD and 7 ns for the DH. Window selection for the channel entrance regions was based on these simulations applying the same selection criteria as above.

Molecular dynamics simulations were performed using the GROMACS package[45,46] applying a combination of the GROMOS96 53a6 force field for gramicidin[47] and the Berger[48] lipid force field. The vdW parameters for K$^+$ and Cl$^-$ ions were taken from Straatsma,[49] while parameters for the D-amino acids were obtained by reflecting the backbone dihedral angle of the respective L-amino acid, and charges for the formyl and ethanolamide groups were assigned according to the parameters from the peptide backbone and the serine residue of the GROMOS 53a6 force field.

In the window simulations, a harmonic potential with a force constant of 4000 kJ mol^{-1} nm^{-2} was employed to restrain the sampled ion around the center of the window. Systems were simulated applying periodic boundary conditions with the temperature coupled to 310 K and pressure coupled semi-isotropically to 1 bar. All H-bonds were constrained using LINCS[50] or SETTLE algorithm,[51] allowing for an integration step size of 2 fs. Pairlists were generated every 10 integration steps. The cutoff for LJ interactions and for short-range electrostatics was set to 1.0 nm, while the long-range electrostatics was treated with the particle-mesh Ewald method (PME).[52] Trajectories were written every picosecond and umbrella sampling data (ion position with respect to the window center) were collected at every integration step. All window simulations were equilibrated for 500 ps; 2.5 ns simulations were
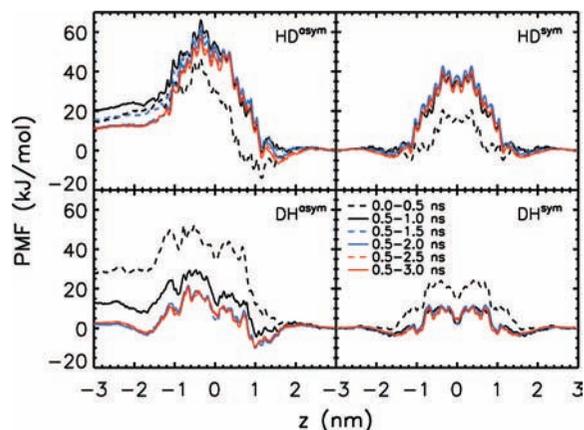
Ion Permeation Through Double-Helical Gramicidin

J. Phys. Chem. B, Vol. 113, No. 10, 2009 **3197**

Figure 2. Time evolution of the asymmetric and symmetric HD (upper panel) and DH (lower panel) PMF profiles. The first 500 ps of the simulations were discarded for subsequent analyses. The 1D-PMF curves are only well defined within the channel constriction zone (approximately $|z| \leq 1.6$ nm).

Figure 3. Comparison of the PMF profiles for K^+ permeation through the gramicidin channel in HD and DH conformation (symmetrized). The 1D-PMF curves are only well defined within the channel constriction zone (approximately $|z| \leq 1.6$ nm). The potassium (K^+) and thallium (Tl^+) profiles of Olah et al.[57] were estimated from the experimental electron density data by $dG = -RT \ln(\rho_{diff}/\rho_{diff}^{max})$, where ρ_{diff} is ρ (ion sample) $- \rho$ (salt-free sample). Hence, the profiles are plotted in arbitrary units. Additional peaks outside of the channel ($|z| = 2nm$) are probably due to small lamellar spacings used in the experiments.

TABLE 1: Comparison of Our PMF Results to Former MD Studies (Energy Values Are Given in kJ mol^{-1})^a

	forcefield	barrier	well depth	total barrier height
this study (HD)	GROMOS96	39.1	—	39.1
			−3.6 at 1.6 nm	
this study (DH)	GROMOS96	10.7	−3.0 at 1.0 nm	13.7
			−3.7 at 1.5 nm	
Allen (HD)^b	CHARMM27	40	−6 at 1.13 nm	46
Bastug (HD)^c	CHARMM27	38	−12 at 1.10 nm	50
Bastug (HD)^d	CHARMM27	33	−17 at 0.97 nm	50
Allen (HD)^b	GROMOS87	63	—	63

^{a} The barrier is measured at the point of largest energy in the channel, typically around the central region; the total barrier height is measured with respect to the internal well depth. ^{b} Values were taken from the uncorrected PMF in Figures 4 and 14 of ref 31. ^{c} Values were taken from ref 55. ^{d} Values were taken from ref 33.

followed for data production. In the WHAM, a sampling bin size of 0.05 Å and tolerance of 0.001 kT were used to check the convergence. Free energies at a distance of 30 Å from the channel center were chosen as the bulk reference. The effect of channel tilting on the free energy profile was estimated by additional window simulations removing the rotational motion of the protein around its center of mass at every integration step. Symmetrized PMF profiles were obtained by averaging the density of states between both sides of the profile.

Note that free energy calculations based on MD simulations are subject to artifacts from the use of PME, periodic boundary conditions, and finite system sizes.[31,53] The error introduced by Ewald summation is inversely proportional to the system size.[54] Concerning lateral periodicity of the membrane-gramicidin system, Allen et al.[31] derived an error of ≈0.1 kJ/mol for the system size used here.

Results

Potential of Mean Force. The PMF for potassium permeation is obtained by averaging over the sampled conformational states for every ion position along the membrane normal. PMF calculations using the umbrella sampling technique require a set of window simulations covering the entire reaction pathway. Depending on the equilibration time of the investigated system and the level of convergence required, each window simulation may take from a few hundred picoseconds[33] to some nanoseconds[31] in order to obtain sufficient statistics.

In this study, each window simulation was run for 3 ns (in total 363 ns of simulation time for each dimer conformation). To test for convergence, the PMF profiles were calculated for different time window length. As shown in Figure 2 (left panel), the root-mean-square deviation (rmsd) between the profiles obtained for the first 500 ps and for the time window between 0.5 and 1.0 ns were 15 (HD) and 17 (DH) kJ/mol. This indicates a rather quick relaxation from the starting configuration in both cases. The first 500 ps of the trajectories were discarded for the PMF calculations to avoid artifacts from equilibration. Despite the structural symmetry of gramicidin, PMF profiles are typically asymmetric due to slow fluctuations not sufficiently sampled in nanosecond simulation, that is, membrane undulations, fluctuations in the lipid packing, or channel tilting. Errors from insufficient sampling are accumulated and may even not be eliminated by extensively long simulation time (see ref 28).
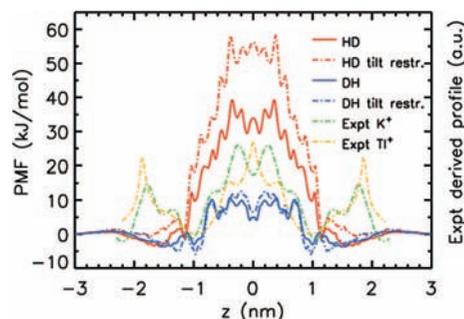
The rmsd between the left and the right side of the potential around the protein center (at $z = 0$) after different simulation time lengths (500 ps, 1 ns, 1.5 ns and so on) were 26, 23, 18, 14, 14 and 15 kJ/mol for HD, and 26, 13, 8, 9, 9 and 8 kJ/mol for DH. This trend of decreasing rmsds implies that the asymmetry is improved at drastically increased simulation times. Typically, the obtained profiles are symmetrized (Figure 2, right panel).

The symmetrized PMF profiles of the two gramicidin conformations show a remarkable difference in stabilizing a K^+ ion along the gramicidin channel. As shown in Figure 3 (solid lines), the HD profile displays a large central barrier of about ≈40 kJ/mol. A wide shallow well is observed at the interface of the channel and the lipid headgroup region. The ion entering the channel experiences a stepwise increase in free energy. Results obtained in this study for the HD conformation are in good agreement with previous free energy calculations for the barrier height. An internal binding site was reported applying the CHARMM and AMBER force fields[31,33,55] (see Table 1); however, for both GROMOS87[31] and for the more recent GROMOS96 (this study), this internal binding site cannot be identified.

In contrast to HD, the DH profile has a much less rugged energy profile with a decreased central barrier of only 14 kJ/mol, at least a factor of 3 lower than for HD. Binding sites both at the channel entrances as well as in the lipid interfacial region are clearly seen. Experimentally, it was observed that gramicidin contains two symmetrically related binding sites at
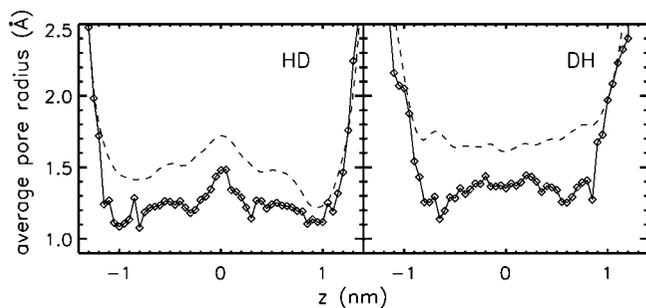
Figure 4. Radius of the channel along the helical axis at the restrained cation positions (solid line). The calculation was done by the HOLE program[86] using a sampling plane distance of 0.25 Å and averaged over snapshots from every 10 ps. The channel radius for the ion-free state is shown as a dashed line.

both ends of the channel.[56-58] However, the exact location and width of the binding sites are slightly different for different cations (e.g., for K^+ and Tl^+, see Figure 3). In our study, the position of the binding site at the channel entrances observed for DH in the simulations are in very good agreement with the binding sites derived from difference electron density profiles between gramicidin in a KCL solution and a salt-free solution[57] (binding sites 10.1 Å from the channel center). Also the central dip in the experimental profile compares favorably with the profile for the DH conformation.

Because the sampled ion is unbound outside the channel, the PMF in the channel entrance region may be dependent on the extent of sampling.[31] For the HD conformation, Bastug et al.[59] showed that the PMF with a restrained potassium differs by ≈1 kT from the unrestrained one. Similarly, for the case of DH, we tested the effect of a flat-bottom lateral restraint (confining the ion radial displacement to within ≈0.8 nm to the center of the channel axis) in the channel entrance region on the PMF profile (data not shown). The resulting PMF profile was similar to the unrestrained profile, the measured total barrier height was increased by less than 1 kJ/mol.

In both equilibration and window simulations, the gramicidin channels are tilted at varying degrees with respect to the membrane normal. HD showed a large average tilt angle of 15° while DH is fairly perpendicular to the membrane plane with a tilt angle of ≈5°. The HD has a channel length of 2.0 nm (measured as the distance between centers of mass of the backbone Cα-atoms forming the last helical turn at the channel ends) as compared to only 1.6 nm for DH. Evidences of transmembrane helix tilting were reported in numerous NMR and infrared spectroscopic studies using gramicidin[60-63] and WALP peptides[64,65] (Leu-Ala core of α-helix flanked by pairs of Trp residues at N- and C-terminals). However, the cause of helix tilting has so far not been fully understood. It was observed as a consequence of membrane hydrophobic mismatch (e.g., membrane thickness, see ref 66 for a review) or the preferential disposition of aromatic residues such as tryptophans in the membrane interface.[64] The magnitude of tilting was found to be affected by the type of lipid headgroup,[63] length of the bilayer hydrophobic core,[65] ordering of the lipid tails,[60,63] peptide length,[67] and packing of aromatic residues.[68] Channel tilting of gramicidin was also reported in previous computational studies,[31,35] but the effect of this tilting on the free energy profiles of ion permeation was not quantified. To answer this question, we performed window simulations with additional restraints on the protein rotational motion, such that the protein helical axis is oriented parallel to the membrane normal.

As to be expected, the PMF profiles obtained from the restrained simulations are more symmetric as compared to the nonrestrained ones. After 3 ns, the rmsd between the left and the right side of the profile decreased to 4 kJ/mol for HD and 3 kJ/mol for DH. As shown in Figure 3 (red and blue dashed−dotted lines), the free energy barrier of the restrained HD is increased by 18 kJ/mol as compared to the flexible HD, while the external binding site is even more shallow. There is no significant change in the ion permeation barrier for the restrained DH, but both internal and external binding sites are slightly shifted inward (to the protein) with a small increase in well depth by 3 and 1 kJ/mol, respectively.

Pore Radius of Gramicidin. Ion translocation through the narrow gramicidin channel occurs in a single-file mode. To some extent, the initial increase of the PMF is due to partial dehydration of the potassium ion upon channel entrance.[69] Inside the narrow channel, the cation is coordinated by two water molecules.[70] The loss of desolvation is partially compensated by attractive electrostatic interactions to the backbone carbonyls[56,58,70,71] which are deflected toward the passing cation. Thus these carbonyls play an important role in coordination of the ion translocation process.

The structural change of the channel in response to the presence of a K^+ ion is reflected by changes in the pore radius. As shown in Figure 4, the DH conformation has a pore with a uniform radius of ≈1.7 Å in the ion-free state. In contrast, the pore is more narrow for the HD at the channel entrances, increasing toward the channel center. In the window simulations, both DH and HD adapt to the bound ion by reorientation of the carbonyls toward the ion, thus resulting in smaller pore radii. Drastic changes close to the channel openings were observed in DH which amounts to a mean reduction of about 50% in the pore radius, reflecting the high flexibility of the double-helical conformation to the conducting ion. As expected from its more narrow pore in the ion-free simulation, the HD is contracted by less than 20% along the channel while maintaining its overall pore shape.

Energy Decomposition. The enthalpic contributions to the PMF can be estimated by analysis of the nonbonded interaction energies of the ion with the protein and the environment. For both HD and DH conformations, the largest contribution to the stabilization (see Figure 5A) of the ion in the pore interior as well as in the binding sites is due to the protein backbone, in agreement with the finding that ion passage is coordinated by the backbone carbonyls. The enhanced backbone contribution for the DH in the channel core is due to the decreased channel length of DH (1.6 nm) as compared to HD (2.0 nm), i.e. the carbonyls have a larger density in the DH core. This attractive contribution is overcompensated by the large positive energies between the potassium ion and the membrane (including the electrolyte) resulting in an energetic barrier for ion permeation. A similar picture was previously reported by Allen et al.[72] for the HD by virtue of the mean force decomposition.

Comparison of the energies of the sampled ion in HD with those in DH (see Figure 5B) reveals more favorable potassium interactions to the phospholipid and the bulk solution for the intertwined double-helical gramicidin. In total, the potassium ion is stabilized by ≈ 90 kJ/mol in DH as compared to HD.

Interestingly, the protein-potassium interactions at the channel entrances are more favorable in HD as compared to DH (≈100 kJ/mol). However, this attractive contribution is outbalanced by a considerably more strong repulsive interaction of the cation to the lipids and the bulk solution in HD (≈180 kJ/mol). These results reveal the determining role of the protein-surrounding lipids (and their hydration shells) in stabilizing the cation at the pore entrance. To investigate this in more detail, we
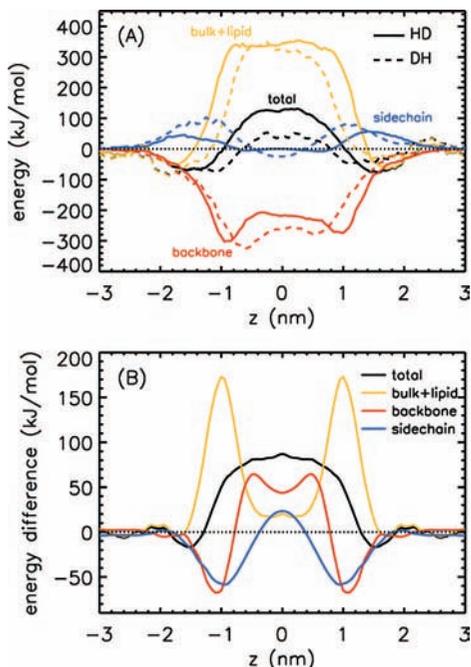
Figure 5. (A) Interaction energies E of the sampled ion with different components of the environment calculated for each umbrella window. E is calculated as the sum of Coulombic and Lennard-Jones interaction energies. The reference energy (leftmost bulk value) is set to zero. Note that the bulk component consists of both water molecules and ions. (B) The difference interaction energy $\Delta E = E_{HD} - E_{DH}$ (symmetrized). Positive values in the plot indicate favorable interactions in DH as compared to HD.
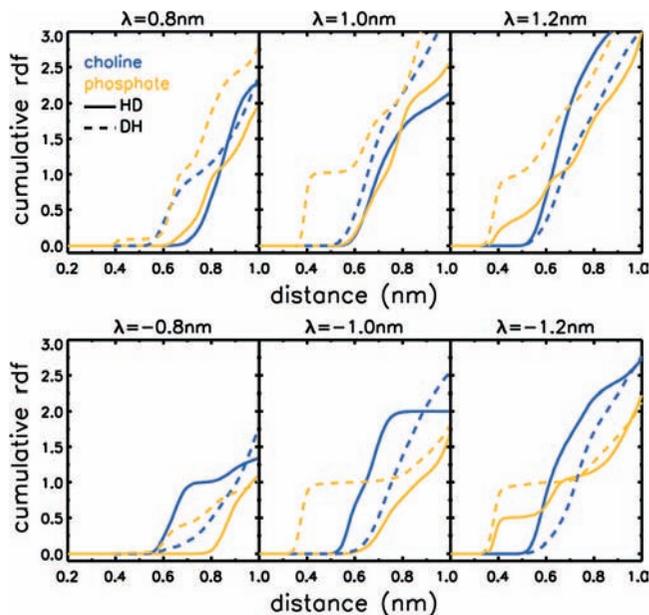

Figure 6. Cumulative radial distribution functions (cdf) of the DMPC choline (blue) and phosphate group (orange) to the sampled potassium ion in umbrella windows (λ indicates the center of the respective window in z dimension). Results for HD are shown as solid lines, those for DH as dashed lines.

calculated the cumulative radial distribution functions (cdf) of the lipid choline and phosphate groups to the potassium ion when the cation is restrained at distances of ± 0.8, ± 1.0, and ± 1.2 nm to the protein center of mass (see Figure 6). It is evident that the phosphate groups (net charge -1) of DH (dashed lines) can reach closer to the pore cation than those of HD. Obviously, the arrangement of the surrounding lipids to
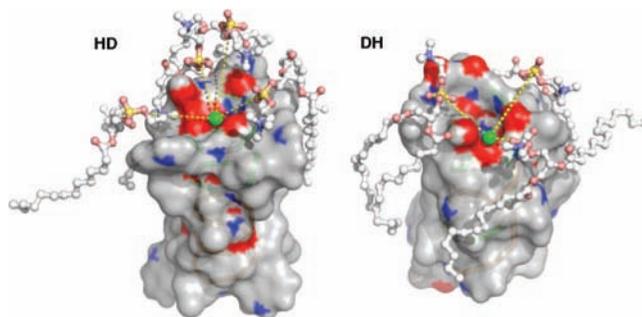

Figure 7. Snapshots of simulations with a potassium ion (colored green) restrained to the channel entrances. Spatially closed lipids are shown in ball-and-stick representation. Yellow dashed lines indicate the interactions between the ions and the lipid phosphorus atoms (colored orange).

the gramicidin is affected by its conformation, as illustrated in Figure 7. In the head-to-head dimer conformation (HD) all tryptophans are located at the channel entrances while they are distributed along the helical axis for the intertwined DH. As seen in the snapshot of HD, the tryptophan cluster at the channel entrances sterically hinders interaction of lipid headgroups with the ion at the channel entrance. In contrast, the DH conformation allows for tighter interaction of the bound ion to surrounding lipids.

PMF with the Modified Potassium−Carbonyl Oxygen Parameters. The GROMOS biomolecular force field used here for the gramicidin was parametrized to reproduce the free enthalpies of solvation in polar and apolar solvents of representative compounds derived from amino acids.[47] In contrast, protein-ion interactions that were not included in the parametrization procedure are typically approximated by conventional combination rules. For these, the Lennard-Jones (LJ) parameters for ions derived in a separate study by Straatsma et al.[49] were chosen. These were fitted to reproduce the free energy of ionic hydration in simple point charge (SPC) water. Therefore, the actual interaction between the ion and the protein infer in this way could possibly be under- or overestimated.

This deficiency of nonpolarizable biomolecular force fields was reported previously in computational studies using the popular CHARMM and AMBER forcefields, and also for the earlier version of GROMOS87.[31,73] Indeed, the microscopic interaction energy between a potassium ion and the model protein NMA in these force fields is larger by 2 (CHARMM) to 37 kJ/mol (GROMOS87)[31] as compared to ab initio studies. For the GROMOS96 force field version 53a6 the deviation to *ab initio* data is decreased to 26 kJ/mol (data not shown) as a result of increased partial charges of the backbone atoms as compared to GROMOS87.

As demonstrated by Allen et al. and Roux et al.[31,73] using the CHARMM force field, a more accurate representation of the protein-ion interactions based on the current potential functions could be obtained by reducing the potassium σ-value of the LJ potential in the interaction to carbonyl oxygens. Here, we tested the effect of similar reductions in the σ-value in the GROMOS96 53a6 force field on the PMF. Two modified potentials were tested by performing window umbrella sampling simulations with $\sigma^{0.95}$ and $\sigma^{0.90}$ (multiplying σ by the indexed factor). As shown in Figure 8, the free energy profiles are sensitive to the change in the potassium LJ parameters, but the influence in the profile was more drastic in HD as compared to DH: The overall profile was shifted downward and broad internal binding sites at the channel entrances emerged. Interestingly, while the total barrier height (the central barrier plus the
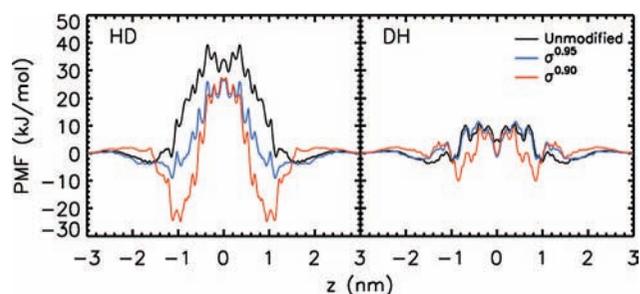
Figure 8. Comparing the PMF profiles obtained with calibrated K⁺−O LJ interactions by adjusting the atomic separation distance σ. The 1D-PMF curves are only well defined within the channel constriction zone (approximately $|z| \leq 1.6$ nm).

well depth) for $\sigma^{0.95}$ was decreased (from 39.1 kJ/mol with the unmodified σ) to 35.5 kJ/mol, further reduction of the σ-value resulted in an increase in the total barrier height (51.9 kJ/mol for $\sigma^{0.90}$) due to an overenhanced stabilization of the binding well. In DH, a scaling of σ by 0.95 had only minor influence on the free energy profile; for $\sigma^{0.90}$, the well depths became more pronounced, similar to the HD case. A conformation-dependent influence of the ion interaction parameter on the PMF profile was expected due to the different distributions of the backbone carbonyls in the channels. The larger effect of the shifted LJ interaction on the HD conformation as compared to DH may be explained by the smaller pore radius of HD and thereby increased sensitivity on the potassium-carbonyl oxygen interaction. For all investigated cases, the total barrier in the HD channel exceeded the DH barrier by 20−30 kJ/mol, underlining the increased stability of potassium in the DH channel as compared to HD.

Discussion and Summary

In this study, we have analyzed the PMF for single potassium ion permeation both through the head-to-head helical dimer conformation and through the double-helical dimer conformation of gramicidin. The shape of the profile and the barrier height of 39.1 kJ/mol obtained for HD using the GROMOS96 53a6 force field is in agreement with earlier studies applying the GROMOS87 and the CHARMM force fields.[31,33,55] However, DH gramicidin embedded in a DMPC lipid bilayer displayed a significantly decreased free energy barrier for potassium ion permeation as compared to HD (13.7 kJ/mol).

Assuming that DH forms a stable channel our result seems to contradict experiments which suggested the HD conformation as the conducting conformation of gramicidin (channel form) while DH was termed the nonchannel conformation.[13,14,16] Conductance experiments by Bamberg et al.[14] and Apell et al.[15] adding bulky negatively charged pyromellityl groups to the N- or C-termini of the peptide observed channel activity only for gramicidin modified at the C-terminus. N-terminal-modified gramicidin, impeding the formation of HD dimers, was suggested to act as a detergent rather than an ion channel. The authors concluded that the gramicidin channel is formed by head-to-head association of the monomers rather than by the DH conformation. However, also the latter conformation was shown to have channel-like properties. For desformylated gramicidin probably predominantly existing in the double-stranded conformation,[37,74] a potassium conductivity of 7 pS was reported (KCL concentration 0.1 M),[74] the same order of magnitude as compared to HD with conductivities of 9−26 pS (KCL concentrations between 0.1 and 1 M[75−77]). It is important to note that the desformylation introduces a positive charge at

the N-terminus which might both decrease the potassium concentration at the channel entrances and modulate the interaction of the gramicidin to the lipid environment (see below). This is in line with a study on cation transport in mitochrondria by gramicidin and by desformylated gramicidin. At high ion concentrations, desformylated gramicidin was reported to be nearly as effective as gramicidin in collapsing the mitochrondrial membrane potential.[78] The ions were suggested to stabilize the channel structure. It should be noted that the charges introduced by desformylation will be screened more effectively at large ion concentrations. Therefore, desformylated gramicidin is probably showing an increased functional similarity to gramicidin in DH conformation at large salt concentrations. The experimental results on desformylated gramicidin together with our finding of a decreased barrier for potassium permeation through DH gramicidin as compared to HD hint at a biological relevance of gA in DH conformation also.

The molecular basis for the decreased free energy barrier for ion permeation through the nonchannel conformation of gramicidin is obtained from a decomposition of the enthalpic contributions to potassium ion stabilization in the gramicidin channel. Neglect of the influence of the lipid and bulk water environment results in a stabilization of the potassium ion in the channel gramicidin (HD) as compared to the nonchannel gramicidin (DH). Thus our results suggest that changes in the lipid environment (and the associated coupled hydration shells) not only change the equilibrium between different gramicidin conformations like those observed experimentally[79] but may have a profound influence on the conductance properties of the channel also without changing the specific channel conformation. Lipids with a modified lipid headgroup are likely to decrease the favorable lipid-ion interaction observed here for the DMPC−DH system. Thus whether the gramicidin in a specific conformation acts as a channel or not is expected to crucially depend on the chosen lipid environment. For that reason, we expect also modifications at the channel entrances to affect channel conductance, for example, by modulating the interaction to the environment. In addition, the channel conductance will also be affected by the tilting angle of the gramicidin which might, for example, probably be affected by the thickness of the hydrophobic core of the chosen membrane environment; for HD a significantly increased free energy barrier was observed for a straigthened channel.

Indole-containing tryptophans along the gramicidin channel have a 2-fold effect on the permeation characteristics of the channel. First, by lipid headgroup interactions they are (co-)responsible for anchoring of the peptide in the membrane and thereby also determine the conformation-dependent arrangement of boundary lipids around the channel (microenvironment). Second, tryptophans assist ion permeation through the channel by favorable electrostatic interactions to the ion, strongly dependent on their localization along the peptide axis and their orientation. The latter was also expected from experiments revealing a reduced conductance of tryptophan-replaced HD channels.[80,81]

We note that the combination of the Berger force field for the phospholipids and the GROMOS96 force field for the protein may overestimate the protein−lipid interaction.[82] The here reported difference in the environment of the gramicidin channel entrances is, however, due to sterical reasons and should thus not severely be influenced by this shortcoming. Although the barrier height for HD applying the recently developed GROMOS96 53a6 force field is comparable to results reported for the CHARMM27 force field, the inner binding site for the HD

Ion Permeation Through Double-Helical Gramicidin

J. Phys. Chem. B, Vol. 113, No. 10, 2009 **3201**

conformation could not be reproduced. Probable reasons for this deficiency are the smaller carbonyl dipole strength used in GROMOS96 as compared to CHARMM27 and the nonideal potassium Lennard-Jones parameters. The strong dependency of the PMF (for HD) on the potassium ion−carbonyl oxygen interaction (see also Allen et al.,[31] a 5% change in the force field parameter decreased the central barrier for HD by more than 10 kJ/mol) underlines the need for consistent force fields in the study of membrane-embedded proteins (see also Siu et al.[83]). Current nonpolarizable force fields only implicitly take polarizability to a different degree into account, the optimal approach to simulate interfaces (protein, membrane, and bulk) in which induced dipole effect has been considered especially important is to use polarizable force fields.[84] Concerning gramicidin, inclusion of membrane polarizability has already been shown to improve the PMF profiles.[25,31,72]

References and Notes

(1) Killian, J. A.; Prasad, K. U.; Hains, D.; Urry, D. W. *Biochemistry* **1988**, *27*, 4848–4855.

(2) LoGrasso, P. V.; Moll, F.; Cross, T. A. *Biophys. J.* **1988**, *54*, 259–267.

(3) Bano, M. C.; Braco, L.; Abad, C. *Biochemistry* **1991**, *30*, 886–894.

(4) Bamberg, E.; Läuger, P. *Biochim. Biophys. Acta* **1974**, *367*, 127–133.

(5) Arndt, H.-D.; Bockelmann, D.; Knoll, A.; Lamberth, S.; Griesinger, C.; Koert, U. *Angew. Chem., Int. Ed.* **2002**, *41*, 4062–4065.

(6) Arseniev, A. S.; Barsukov, I. L.; Bystrov, V. F. *FEBS Lett.* **1985**, *180*, 33–39.

(7) Ketchem, R. R.; Roux, B.; Cross, T. A. *Structure* **1997**, *5*, 1655–1669.

(8) Lomize, A. L.; Orekhov, V. Y.; Arseniev, A. S. *Bioorg. Chemistry* **1992**, *18*, 182–200.

(9) Burkhart, B. M.; Li, N.; Langs, D. A.; Pangborn, W. A.; Duax, W. L. *Proc. Natl. Acad. Sci. U.S.A.* **1998**, *95*, 12950–12955.

(10) Cornell, B. *J. Bioenerg. Biomembr.* **1987**, *19*, 655–676.

(11) Wallace, B. A. *J. Struct. Biol.* **1998**, *121*, 123–141.

(12) Kelkar, D. A.; Chattopadhyay, A. *Biochim. Biophys. Acta* **2007**, *1768*, 2011–2025.

(13) Urry, D. W.; Goodall, M. C.; Glickson, J. D.; Mayers, D. F. *Proc. Natl. Acad. Sci. U.S.A.* **1971**, *68*, 1907–1911.

(14) Bamberg, E.; Apell, H. J.; Alpes, H. *Proc. Natl. Acad. Sci. U.S.A.* **1977**, *74*, 2402–2406.

(15) Apell, H. J.; Bamberg, E.; Alpes, H.; Läuger, P. *J. Membr. Biol.* **1977**, *31*, 171–188.

(16) Weinstein, S.; Wallace, B. A.; Blout, E. R.; Morrow, J. S.; Veatch, W. *Proc. Natl. Acad. Sci. U.S.A.* **1979**, *76*, 4230–4234.

(17) Wallace, B. A.; Veatch, W. R.; Blout, E. R. *Biochemistry* **1981**, *20*, 5754–5760.

(18) Andersen, O. S.; Apell, H.-J.; Bamberg, E.; Busath, D. D.; Koeppe, R. E.; Sigworth, F. J.; Szabo, G.; Urry, D. W.; Woolley, A. *Nat. Struct. Biol.* **1999**, *6*, 609.

(19) Cross, T. A.; Arseniev, A.; Cornell, B. A.; Davis, J. H.; Killian, J. A.; Koeppe, R. E.; Nicholson, L. K.; Separovic, F.; Wallace, B. A. *Nat. Struct. Biol.* **1999**, *6*, 610–611.

(20) Burkhart, B. M.; Duax, W. L. *Nat. Struct. Biol.* **1999**, *6*, 611–612.

(21) Levitt, D. G. *Biophys. J.* **1978**, *22*, 209–219.

(22) Monoi, H. *Biophys. J.* **1991**, *59*, 786–794.

(23) Edwards, S.; Corry, B.; Kuyucak, S.; Chung, S.-H. *Biophys. J.* **2002**, *83*, 1348–1360.

(24) Nadler, B.; Hollerbach, U.; Eisenberg, R. S. *Phys. Rev. E* **2003**, *68*, 021905.

(25) Åqvist, J.; Warshel, A. *Biophys. J.* **1989**, *56*, 171–182.

(26) Mamonov, A. B.; Coalson, R. D.; Nitzan, A.; Kurnikova, M. G. *Biophys. J.* **2003**, *84*, 3646–3661.

(27) Dorman, V. L.; Jordan, P. C. *Biophys. J.* **2004**, *86*, 3259–3541.

(28) Kato, M.; Warshel, A. *J. Phys. Chem. B* **2005**, *109*, 19516–19522.

(29) Allen, T. W.; Andersen, O. S.; Roux, B. *J. Am. Chem. Soc.* **2003**, *125*, 9868–9877.

(30) Braun-Sand, S.; Burykin, A.; Chu, Z. T.; Warshel, A. *J. Phys. Chem. B* **2005**, *109*, 583–592.

(31) Allen, T. W.; Andersen, O. S.; Roux, B. *Biophys. J.* **2006**, *90*, 3447–3468.

(32) Liu, Z.; Xu, Y.; Tang, P. *J. Phys. Chem. B* **2006**, *110*, 12789–12795.

(33) Bastug, T.; Kuyucak, S. *Biophys. J.* **2006**, *90*, 3941–3950.

(34) Bastug, T.; Kuyucak, S. *J. Chem. Phys.* **2007**, *126*, 105103.

(35) Qin, Z.; Tepper, H. L.; Voth, G. A. *J. Phys. Chem. B* **2007**, *111*, 9931–9939.

(36) Fabritiis, G. D.; Coveney, P. V.; Villá-Freixa, J. *Proteins* **2008**, *73*, 185–194.

(37) de Groot, B. L.; Tieleman, D. P.; Pohl, P.; Grubmüller, H. *Biophys. J.* **2002**, *82*, 2934–2942.

(38) Siu, S. W. I.; Böckmann, R. A. *J. Struct. Biol.* **2007**, *157*, 545–556.

(39) Ketchem, R. R.; Lee, K. C.; Huo, S.; Cross, T. A. *J. Biomol. NMR* **1996**, *8*, 1–14.

(40) Kucerka, N.; Liu, Y.; Chu, N.; Petrache, H. I.; Tristram-Nagle, S.; Nagle, J. F. *Biophys. J.* **2004**, *88*, 2626–2637.

(41) Kirkwood, J. G. *J. Chem. Phys.* **1935**, *3*, 300.

(42) Roux, B. *Comput. Phys. Commun.* **1995**, *91*, 275–282.

(43) Kumar, S.; Bouzida, D.; Swendsen, R. H.; Kollman, P. A.; Rosenberg, J. M. *J. Comput. Chem.* **1992**, *13*, 1011–1021.

(44) Chiu, S.-W.; Subramaniam, S.; Jakobsson, E. *Biophys. J.* **1999**, *76*, 1939–1950.

(45) Berendsen, H. J. C.; van der Spoel, D.; van Drunen, R. *Comput. Phys. Commun.* **1995**, *91*, 43–56.

(46) Lindahl, E.; Hess, B.; van der Spoel, D. *J. Mol. Model.* **2001**, *7*, 306–317.

(47) Oostenbrink, C.; Villa, A.; Mark, A. E.; van Gunsteren, W. F. *J. Comput. Chem.* **2004**, *25*, 1656–1676.

(48) Berger, O.; Edholm, O.; Jähnig, F. *Biophys. J.* **1997**, *72*, 2002–2013.

(49) Straatsma, T. P.; Berendsen, H. J. C.; Postma, J. P. M. *J. Chem. Phys.* **1986**, *85* (11), 6720–6727.

(50) Hess, B.; Bekker, H.; Berendsen, H. J. C.; Fraaije, J. G. E. M. *J. Comput. Chem.* **1997**, *18*, 1463–1472.

(51) Miyamoto, S.; Kollman, P. A. *J. Comput. Chem.* **1992**, *13*, 952–962.

(52) Darden, T.; York, D.; Pedersen, L. *J. Chem. Phys.* **1993**, *98*, 10089–10092.

(53) Warshel, A.; Sharma, P. K.; Kato, M.; Parson, W. W. *Biochim. Biophys. Acta* **2006**, *1764*, 1647–1676.

(54) Figueirido, F.; Levy, R. M.; Zhou, R.; Berne, J. *J. Chem. Phys.* **1997**, *106*, 9835–9849.

(55) Bastug, T.; Patra, S. M.; Kuyucak, S. *Chem. Phys. Lipids* **2006**, *141*, 197–204.

(56) Koeppe, R. E.; Berg, J. M.; Hodgson, K. O.; Stryer, L. *Nature* **1979**, *279*, 723–725.

(57) Olah, G. A.; Huang, H. W.; Liu, W.; Wu, Y. *J. Mol. Biol.* **1991**, *218*, 847–858.

(58) Urry, D. W.; Prasad, K. U.; Trapane, T. L. *Proc. Natl. Acad. Sci. U.S.A.* **1982**, *79*, 390–394.

(59) Bastug, T.; Kuyucak, S. *J. Chem. Phys.* **2008**, *128*, 227102.

(60) Okamura, E.; Umemura, J.; Takenaka, T. *Biochim. Biophys. Acta* **1986**, *856*, 68–75.

(61) Prosser, R. S.; Davis, J. H. *Biophys. J.* **1994**, *66*, 1429–1440.

(62) Ulrich, W.-P.; Vogel, H. *Biophys. J.* **1999**, *76*, 1639–1647.

(63) Kóta, Z.; Páli, T.; Marsh, D. *Biophys. J.* **2004**, *86*, 1521–1531.

(64) van der Wel, P. C. A.; Strandberg, E.; Killian, J. A.; Koeppe, R. E. *Biophys. J.* **2002**, *83*, 1479–1488.

(65) Strandberg, E.; Özdirekcan, S.; Rijkers, D. T. S.; van der Wel, P. C. A.; Koeppe, R. E.; Liskamp, R. M. J.; Killian, J. A. *Biophys. J.* **2004**, *86*, 3709–3721.

(66) Killian, J. A. *Biochim. Biophys. Acta* **1998**, *1376*, 401–416.

(67) Sengupta, D.; Meinhold, L.; Langosch, D.; Ullmann, G. M.; Smith, J. C. *Proteins* **2005**, *58*, 913–922.

(68) Ulmschneider, M. B.; Sansom, M. S. P.; Nola, A. D. *Biophys. J.* **2006**, *90*, 1650–1660.

(69) Andersen, O. S.; Koeppe, R. E.; Roux, B. *IEEE Trans. Nanobiosci.* **2005**, *4*, 10–20.

(70) Mackay, D. H.; Berens, P. H.; Wilson, K. R.; Hagler, A. T. *Biophys. J.* **1994**, *46*, 229–248.

(71) Allen, T. W.; Bastug, T.; Kuyucak, S.; Chung, S.-H. *Biophys. J.* **2003**, *84*, 2159–2168.

(72) Allen, T. W.; Andersen, O. S.; Roux, B. *Proc. Natl. Acad. Sci. U.S.A.* **2004**, *101*, 117–122.

(73) Roux, B.; Bernéche, S. *Biophys. J.* **2002**, *82*, 1681–1684.

(74) Saparov, S. M.; Antonenko, Y. N.; Koeppe, R. E.; Pohl, P. *Biophys. J.* **2000**, *79*, 2526–2534.

(75) Hladky, S. B.; Haydon, D. A. *Biochim. Biophys. Acta* **1972**, *274*, 294–312.

(76) Urry, D. W.; Alonso-Romanowski, S.; Venkatachalam, C. M.; Harris, R. D.; Prasad, K. U. *Biochem. Biophys. Res. Commun.* **1984**, *118*, 885–893.

(77) Busath, D. D.; Thulin, C. D.; Hendershot, R. W.; Phillips, L. R.; Maughan, P.; Cole, C. D.; Bingham, N. C.; Morrison, S.; Baird, L. C.; Hendershot, R. J.; Cotten, M.; Cross, T. A. *Biophys. J.* **1998**, *75*, 2830–2844.

(78) Rottenberg, H.; Koeppe-II, R. E. *Biochemistry* **1989**, *28*, 4361–4367.

(79) Mobashery, N.; Nielsen, C.; Andersen, O. S. *FEBS Lett.* **1997**, *412*, 15–20.

(80) Becker, M. D.; Greathouse, D. V.; Koeppe-II, R. E.; Andersen, O. S. *Biochemistry* **1991**, *30*, 8830–8839.

(81) Andersen, O. S.; Greathouse, D. V.; Providence, L. L.; Becker, M. D.; Koeppe, R. E. *Biophys. J.* **1998**, *120*, 5142–5146.

(82) Tieleman, D. P.; MacCallum, J. L.; Ash, W. L.; Kandt, C.; Xu, Z.; Monticelli, L. *J. Phys.: Condens. Matter* **2006**, *18*, S1221−S1234.

(83) Siu, S. W. I.; Vacha, R.; Jungwirth, P.; Böckmann, R. A. *J. Chem. Phys.* **2008**, *128*, 125103.

(84) Jungwirth, P.; Tobias, D. *J. Chem. Rev.* **2006**, *106*, 1259–1281.

(85) DeLano, W. L. http://www.pymol.org (accessed 2002).

(86) Smart, O. S.; Neduvelil, J. G.; Wang, X.; Wallace, B. A.; Sansom, M. S. P. *J. Mol. Graphics* **1996**, *14*, 354–360.